RSC Advances

ROYAL SOCIETY OF CHEMISTRY

www.rsc.org/advances

Monolayer MoS_2 quantum dots as catalysts for efficient hydrogen evolution

Wen Qiao[1], Shiming Yan[1, 2], Xueyin Song[1], Xing Zhang[1], Yuan Sun[1], Xing Chen[1], Wei Zhong[1*], Youwei Du[1]

[1] *Collaborative Innovation Center of Advanced Microstructures, National Laboratory of Solid State Microstructures and Jiangsu Provincial Laboratory for NanoTechnology, Nanjing University, Nanjing , 210093, China*

[2]*College of Science, Henan University of Technology, Zhengzhou 450001, P. R. China*

Abstract

Monolayer MoS_2 quantum dots (QDs) with lateral size around 3 nm were prepared through an effective multi-exfoliation based on lithium (Li) intercalation. The effects of the number of exfoliation on the microstructures and electrocatalytic activities of hydrogen evolution reaction (HER) for MoS_2 nanosheets were examined. The lateral size of the nanosheets decreases rapidly with incerasing the number of exfoliation. The obtained monolayer MoS_2 QDs exhibit improved HER catalytic activities with a low overpotential of approximately 120 mV and a relatively small Tafel slope of 69 mV dec^{-1}. Both the ultrathin structure and the abundance of exposed active edge sites make monolayer MoS_2 QDs a promising HER electrocatalyst for practical application.

* Corresponding author: wzhong@nju.edu.cn

Introduction

Hydrogen is a cleanest energy and serves as one of the most promising candidates for replacing fossil fuels in the future.[1] Efficient hydrogen production based on electrocatalytic water-splitting has attracted growing attention.[2, 3] Although Pt-group metals are the most efficient electrocatalysts for hydrogen evolution reaction (HER), [4, 5] the high cost and global low availability prevent their widespread application.[6, 7, 8] Therefore, the development of an economic and earth-abundant HER catalyst remains a major challenge.[9, 10, 11]

Over the past few years, nano-scaled molybdenum disulfide (MoS_2) has been shown a promising electrocatalysts for the HER owing to its high activity and chemical stability, as well as low price.[12-20] Considerable efforts have been made to investigating and optimizing the catalytic activities of MoS_2. Both theoretical [21] and experimental [22] studies have shown that the HER activity of MoS_2 is highly dependent on the sites located along the exposed edges of MoS_2 plates, while the basal planes are catalytically inert. Thus, increasing the number of edge sites is an effective strategy to enhance the catalytic activity.[23-28] Furthermore, MoS_2 possesses a layered structure composed of S-Mo-S triple layers which are weakly bonded by van der Waals forces.[29] This two-dimensional (2D) structure offers 2D permeable channels for electrons transport [30, 31] while the interlayer potential barrier in the vertical direction of MoS_2 layers hinders the jumping of electrons.[32] Thus, the conductivity parallel to the plane is two orders of magnitude higher than that between the adjacent layers.[14, 33] Considering about these, decreasing the number of layers to a few, even to only one (*i.e.* monolayer) would improve the conductivity and thus enable a fast electron transport during the catalytic process.

Compared with other MoS_2 nanostructures, zero-dimensional monolayer MoS_2 QDs satisfy both the large edge-to-volume ratio and high in-plane electron transport together, which are beneficial to the improved HER activity. Up to now, the chemical exfoliation [34, 35] based on Li intercalation is the most suitable route for the large scale production of monolayer MoS_2

nanosheets. In our previous work,[36] we noticed that the lateral size of the MoS_2 nanosheets decreased remarkably after the chemical exfoliation of the MoS_2 bulk material with Li intercalation. If the samples were repeatedly exfoliated with Li intercalation, a plenty of monolayer MoS_2 nanosheets with small lateral size could be produced. Therefore, the multiply exfoliation based on Li intercalation would be an efficient route to synthesis monolayer MoS_2 QDs in large scale.

In this paper, a multi-exfoliation route was used to prepare monolayer MoS_2 quantum dots with the lateral size around 3 nm. The lateral size of MoS_2 nanosheets decreases obviously from hundreds nanometers to several nanometers with the increasing exfoliation numbers, and a large number of MoS_2 QDs are obtained after the third exfoliation. The MoS_2 QDs exhibit improved electrocatalytic activity for HER with low overpotential and small Tafel slope, which mainly resulted from the enhancement of exposed active edges of monolayer MoS_2 QDs.

Experimental section

Multiple Li intercalation was used to prepare monolayer MoS_2 quantum dots (QDs) from the bulk 2H-MoS_2 (M-bulk) powder. The first exfoliation was achieved by immersing 1 g of pristine MoS_2 powder in 10 mL of 2.2M n-butyl lithium solution in hexane for 2 days in a flask filled with argon gas. The Li_xMoS_2 was retrieved by filtration and washed repeatedly with hexane to remove excess lithium and organic residues. Exfoliation was achieved immediately afterward by ultrasonicating Li_xMoS_2 in water for 1h at the power of 180 W. Flocculation occurred rapidly when the pH value was reduced to 2 with the addition of hydrochloric acid. The mixture was washed with water and centrifuged several times to obtain neutral flocculation with a pH of 7. The flocculation was dried at 100 ℃ in a vacuum drying oven and then the dried re-stacked MoS_2 nanosheets for the first exfoliation (M-1) were obtained. The re-stacked MoS_2 nanosheets were undergone continually the second (M-2) and third (M-3) exfoliation with Li-intercalation by repeating the above experimental procedures. After the third

exfoliation, the resulting mixture was centrifuged several times at 2000 rpm to remove un-exfoliated material. Purification for eliminating lithium hydroxide (LiOH) was carried out with a dialysis bag (Molecular weight cut-off: 1 kDa) for 3 h. The as-prepared MoS_2 QDs were collected by further centrifugation at 12000 rpm for 20 min and then dried in vacuum oven at 40 ℃ prior the further use.

The morphology of each exfoliated samples and MoS_2 QDs was examined by transmission electron microscopy (TEM) (Model JEOL-2010, Japan) operated at an accelerating voltage of 120 kV. Scanning electron microscopy (SEM) images were obtained by a field-emission instrument (FEI Sirion200). Atomic force microscope (AFM) images were taken using Scanning Probe Microscopy (Veeco Dimension V, USA). The crystal structure was characterized by X-ray diffraction (XRD) using a Philips X'pert diffractometer with Cu Kα radiation. UV-vis absorbance spectra were recorded using a spectrophotometric system of Double beam UV visible spectrophotometer (TU-1901). Raman spectroscopic investigations were performed on a J.Y. HR-800 confocal spectrograph (Horiba, Japan) with an excitation wavelength of 532 nm. X-ray photoelectron spectrum (XPS) was measured on a PHI5000 VersaProbe (ULVAC-PHI, Japan) using Al Kα radiation.

Electrochemical measurements were carried out with a computer-controlled potentiostat (CHI660D) in a standard three-electrode system with 0.5 M H_2SO_4 as electrolyte. A Pt wire and an Ag/AgCl (in 3.5 M KCl solution) electrode were used as counter and reference electrode respectively. A glassy carbon (GC) electrode modified by MoS_2 as the working electrode. The working electrodes were prepared as follows: (1) all materials (M-bulk, M-1, M-2, M-3 and M-QDs powder) were dispersed in N, N-dimethylformamide (DMF) at concentration of 5 mg/mL. (2) 3 μL portion of the MoS_2 suspension was deposited on a previously polished glassy carbon electrode and 3 μL of Nafion solution (0.5 wt%) was coated after the suspension was dried at room temperature. Linear sweep voltamperometry was performed in 0.5 M H_2SO_4

solution with a scan rate of 5 mV s^{-1}. AC impedance spectra were performed in the same configuration from 10^6-0.01 Hz with an AC voltage of 5 mV.

Results and Discussion

The multi-exfoliation through Li intercalation of bulk MoS_2 (about 10 μm in lateral size as shown in Figure S1) was employed to prepare monolayer MoS_2 QDs. To clearly characterize the variety of morphology, transmission electron microscopy (TEM) and atomic force microscope (AFM) were performed on the MoS_2 nanosheets after each exfoliation. As we can see from Figure 1a, the lateral sizes of the exfoliated MoS_2 sheets after the first chemical exfoliation distribute in the range of 100-800 nm with an average size about 250 nm, significantly smaller than that of the bulk MoS_2 (about 10 μm, shown in Figure S1). The firstly exfoliated MoS_2 suspension was dried in vacuum drying oven to form the re-stacked MoS_2 nanosheets, which are used for the second Li-intercalated exfoliation. After the second exfoliation, the lateral sizes of the MoS_2 nanosheets are between 10-100 nm with an average size about 30 nm, as shown in Figure 1b. The third Li-intercalation of the dried MoS_2 nanosheets and the following exfoliation result in a further decrease in the size of MoS_2 nanosheets reaching to 2-10 nm, as shown in Figure 1c. The lateral size of MoS_2 nanosheets decreased approximately by 10 times after each exfoliation. The obvious lateral size variation is further confirmed by the AFM images (see Figure 1d-f). As we can see from Figure S2, after the third exfoliation, the number of MoS_2 nanosheets less than 10 nm in lateral size reaches 94% which is much greater than that of the second exfoliation (~4%), meaning that the third time exfoliation can effective preparation small MoS_2 QDs in large scale. The height profiles overlaid on the AFM images show that the thickness of most of the MoS_2 nanosheets after each time exfoliation is ~1 nm, indicating that the MoS_2 nanosheets are monolayer.

The crystal structures of the bulk MoS_2 (M-bulk), re-stacked MoS_2 nanosheets for each exfoliation and the as-prepared MoS_2 QDs (M-QDs) were systematically investigated by X-ray

diffraction (XRD) measurements, as shown in Figure 2. The XRD spectrum of pristine 2H-MoS_2 shows a very strong diffraction peak at $2\theta = 14.4°$ and two weak peaks at $2\theta = 39.6°$ and 49.8°, which are assigned to (002), (103) and (105) faces, respectively (JCPDF 65-0160). It is noteworthy that the peaks of the (002) reflection of dried MoS_2 nanosheets are significantly broadened and weakened with increasing exfoliated number, indicating the decrease of the lateral size and the highly exfoliated nature.[17] The dried M-QDs powder was also characterized by means of XRD, showing very weak XRD signals. This could be due to the ultrafine size of monolayer MoS_2 QDs, which re-stack disorderly during the process of drying, and almost no order crystal face is formed.

To confirm the structure and thickness of the MoS_2 QDs, TEM and AFM analysis were also analyzed. Figure 3a shows a TEM image of the uniform MoS_2 QDs. The lateral size of MoS_2 QDs ranges from 1.5 to 4.5 nm, with an average value of approximately 2.9 nm (inset in Figure 3a). The ordered lattice fringes in high-resolution TEM (HRTEM) images suggest the QDs are well-crystallized (Figure 3b). The d-spacing of MoS_2 QDs is about 2.7 Å, which corresponds to the (100) faces of MoS_2 crystals. From AFM images (Figure 3c and 3d), it can be seen that similar to the as-exfoliated samples most of the MoS_2 QDs are monolayer.

The chemical states of Mo and S in the MoS_2 QDs were analyzed by X-ray photoelectron spectroscopy (XPS) measurement. The high-resolution XPS of the MoS_2 QDs in the Mo 3d region is shown in Figure S3a. Two characteristic peaks arising from 229.4 and 232.5 eV can be attributed to the Mo $3d_{5/2}$ and $3d_{3/2}$ binding energies for a Mo (IV) oxidation state.[37] The high binding energy peak (235.8 eV) is attributed to Mo (VI) oxidation state, [14] as commonly observed when the MoS_2 sample is exposed to air for a long time. In the S 2p spectrum (Figure S3b), two peaks are observed at 162.1 and 163.3 eV corresponding to S $2p_{3/2}$ and S $2p_{1/2}$ of MoS_2, respectively.[25] These data indicate that the sample is mainly composed of MoS_2 QDs. Raman spectroscopy further confirmed the structure of MoS_2 QDs (Figure S4) with the

appearance of two distinguished peaks near 382 and 405 cm^{-1} for the in-plane (E^1_{2g}) and vertical plane (A_{1g}) vibrations modes, respectively.[38] The peak for the A_{1g} mode of MoS_2 QDs is blue shift by 3.2 cm^{-1} compared to that of bulk MoS_2. As a result, the peak spacing between E^1_{2g} and A_{1g} of the MoS_2 QDs (22.5 cm^{-1}) is much less than that in bulk MoS_2 (25.7 cm^{-1}), indicating the monolayer structure.[14]

The optical properties of all samples were characterized by absorption spectra. Figure S5 shows the UV-vis spectra of MoS_2 nanosheets and QDs. For the large MoS_2 nanosheets, there are four clear peaks at 679, 625, 448, and 402 nm, assigned to A, B, C, and D excitonic features.[17, 38, 39] These four peaks become blue shift with increasing the exfoliated number, indicating that the lateral size of MoS_2 nanosheets decreases with the exfoliated number. While on the spectra of monolayer MoS_2 QDs, these four characteristic peaks disappear; and instead, two absorption bands edges peaked at ~290 and ~230 nm are observed. It is thus suggested that the option absorption of monolayer MoS_2 QDs exhibits a strong blue shift when the lateral dimensions of the MoS_2 nanostructures reduce to several nanometers, due to the quantum confinement effect.[17, 39, 40]

To investigate the electrocatalytic HER activity of monolayer MoS_2 QDs, the glassy carbon (GC) electrode was modified using MoS_2 QDs for linear sweep voltammetry (LSV) measurements in 0.5 M H_2SO_4 solution using a typical three-electrode system. As a comparison, similar measurements were also performed on GC electrode modified by bulk MoS_2 and each exfoliation MoS_2 materials. The results are also compared with bare GC and a commercial Pt wire electrode. As shown in Figure 4a, the Pt catalyst exhibits extremely high HER catalytic activity with a near zero onset overpotential (η). Bulk MoS_2 displays extremely weak HER performance with a high onset overpotential ~390 mV and a weak cathodic current density. After the multiply exfoliation, the MoS_2 materials show an enhanced performance in HER activity. The onset overpotential decreases, while the current density increases gradually at a

given potential with increasing the exfoliation times, as shown in Table 1 and Figure 4a. In contrast, the MoS_2 QDs possess much higher HER activity with a small onset overpotential ~120 mV, suggesting the superior HER activity. Furthermore, the MoS_2 QDs exhibit an extremely high cathodic current density of 35 mA/cm^2 at η = -300 mV, which is much larger than that of bulk MoS_2 and other three MoS_2 materials. It shows that the cathodic current density obtained here is about two times larger than the results of MoS_2 QDs synthesized by hydrothermal method [14] and electrochemical methods [19] reported recently.

The Tafel slope, determined by Tafel plots where their linear portions are fit to the Tafel equation ($\eta = b\log j + a$, where j is the current density and b is the Tafel slope), reflects the intrinsic properties of the electrocatalyst materials.[14, 17] The Tafel slope of the Pt catalyst is ~30 mV per decade (Figure 4b), very similar to that reported in the previous work.[15, 41] For monolayer MoS_2 QDs, the Tafel slope is 69 mV dec^{-1}, much smaller than that of bulk MoS_2 (190 mV dec^{-1}) and each exfoliation MoS_2 nanosheets (101-181 mV dec^{-1}). A smaller Tafel slope means a faster increase of HER rate with the increasing potential.[42] Therefore, the smallest slope of MoS_2 QDs suggests the presence of a large number of active catalytic sites resulting in improved reaction kinetics. Another important HER rate parameter, namely the exchange current density, j_0, can be estimated by extrapolating the Tafel plot and was found to be 1.79 × 10^{-5} Acm^{-2} for the MoS_2 QDs, as shown in table 1. The high exchange current density obtained also reflects the abundance in the number of active sites.

To directly investigate the effect of active sites brought in by the ultrafine MoS_2 QDs, the turnover frequency (TOF) was then calculated from current density,[22, 43] as shown in Figure 4c and Supporting Information. The calculated TOF based on j_0 (Table 1) for the MoS_2 QDs reaches 4.81 x 10^{-2} s^{-1}, which is much higher than the value 0.64 x 10^{-2} s^{-1} for the bulk MoS_2, suggesting the improved intrinsic activity of the active sites. Electrochemical impedance spectra (EIS) were performed to confirm the conductivity of MoS_2 catalysts. The Nyquist plots

of the samples are given in Figure S6. As we can see from Nyquist plots, the charge-transfer resistance (R_{ct}) of the samples first decreases and then increases with increasing the number of exfoliation. The charge-transfer resistance of bulk MoS_2 is about 4.3 kΩ, while for the sample of M-1, the charge transfer resistance is obviously reduced to 1.6 kΩ. After the second exfoliation, the charge-transfer resistance gradually increases, reaching to 4.1 kΩ for MoS_2 QDs. It can be seen that the reduction of the number of layers could decrease the charge-transfer resistance.[32] Nevertheless, with the decrease of the size of the nanosheets, the amount of the interface between the nanosheets is increased, which hinders the transmission of electrons. Therefore, the charge-transfer resistance of MoS_2 QDs is larger than that of the large MoS_2 nanosheets. Thus, the enhanced catalytic activity of MoS_2 QDs may be correlated mainly with the abundant edge sites of MoS_2 QDs. The increased perimeter/basal ratio shown in Figure 4d indicates that the multiply exfoliation route can efficiently cut the large MoS_2 nanosheets into small nanosheet, resulting in a great deal of exposed edge sites of the materials.

Apart from the HER activity, long-term stability of the catalyst is also a key criterion to evaluate the performance of the material. Figure 5 displays the polarization curves of monolayer MoS_2 QDs before and after 2000 cycles. The negligible loss of the cathodic current indicates the favorable stability of the monolayer MoS_2 QDs in electrochemical process.

Conclusions

In conclusion, an effective method is testified for preparation of monolayer MoS_2 QDs with a lateral size around 3 nm, from their bulk MoS_2 material, using a multi-exfoliation via lithium intercalation process. The lateral size of the nanosheets decreases rapidly with increasing the number of exfoliation. After the third exfoliation, a large number of monolayer MoS_2 QDs is formed. Compared with MoS_2 nanosheets, monolayer MoS_2 QDs exhibit improved HER activity with a low overpotential ~ 120 mV, large cathodic current, and a small Tafel slope ~ 69 mV/ decade. The abundant active edge sites of monolayer MoS_2 QDs lead to the excellent

catalytic performance toward the HER. This multiply exfoliation method present a facile pathway for large-scale synthesis of transition metal dichalcogenides QDs for their emerging application in energy conversion technologies and other technological applications.

Acknowledgements

This work was supported by the National Natural Science Foundation of China (Grant Nos.11474151 and 11174132), the National Key Project for Basic Research (Grant Nos. 2011CB922102 and 2012CB932304), and PAPD, People's Republic of China.

References

[1] J. A. Turner, *Science*, 2004, 305, 972-974.

[2] T. E. Mallouk, *Nat. Chem.*, 2013, 5, 362-363.

[3] J. K. Norskov and C. H. Christensen, *Science*, 2006, 312, 1322-1323.

[4] F. Raimondi, G. G. Scherer, R. Kotz and A. Wokaun, *Angew. Chem., Int. Ed.*, 2005, 44, 2190-2209.

[5] R. Tolle and A. Otto, *Surf. Sci.*, 2005, 597, 110-118.

[6] M. Arenz, V. Stamenkovic, T. J. Schmidt, K. Wandelt, P. N. Ross and N. M. Markovic, *Surf. Sci.*, 2002, 506, 287-296.

[7] B. Fang, M. Kim, J. Kim, M. Song, Y. Wang, H. Wang, D. Wilkinson and J. S. Yu, *J. Mater. Chem.*, 2011, 21, 8066-8073.

[8] N. R. Elezovic, L. Gajic-Krstajic, V. Radmilovic, L. Vracar and N. V. Krstajic, *Electrochim. Acta*, 2009, 54, 1375-1382.

[9] M. G.Walter, E. L. Warren, J. R. Mckone, S. W. Boettcher, Q. X. Mi, E. A. Santori and N. S. Lewis, *Chem. Rev.*, 2010, 110, 6446-6473.

[10] Y. Li and G. A. Somorjai, *Nano Lett.*, 2010, 10, 2289-2295.

[11] Y. D. Hou, B. L. Abrams, P. C. K. Vesborg, M. E. Bjorketun, K. Herbst, L. Bech, A. M. Stti, C. D. Damsgaard, T. Pedersen, O. Hansen, J. Rossmeisl, S. Dahl, J. K. Norskov and I. Chorkendorff, *Nat. Mater.*, 2011, 10, 434-438.

[12] Y. Yan, B. Y. Xia, X. Ge, Z. Liu, J. Y. Wang and X. Wang, *ACS Appl. Mater. Interfaces*, 2013, 5, 12794-12798.

[13] Z. Wu, B. Fang, Z. Wang, C. Wang, Z. Liu, F. Liu, W. Wang, A. Alfantazi, D. Wang and D. P. Wilkinson, *ACS Catal.*, 2013, 3, 2101-2107.

[14] X. Ren, L. Pang, Y. Zhang, X. Ren, H. Fanac and S. Liu, *J. Mater. Chem. A*, 2015, 3, 10693-10697.

[15] J. Xie, J. Zhang, S. Li, F. Grote, X. Zhang, H. Zhang, R. Wang, Y. Lei, B. Pan and Y. Xie, *J. Am. Chem. Soc.*, 2013, 135, 17881-17888.

[16] D. Voiry, M. Salehi, R. Silva, T. Fujita, M. Chen, T. Asefa, V. B. Shenoy, G. Eda and M. Chhowalla, *Nano Lett.*, 2013, 13, 6222-6227.

[17] S. Xu, D. Li and P. Wu, *Adv. Funct. Mater.*, 2015, 25, 1127-1136.

[18] D. Merki, S. Fierro, H. Vrubel and X. Hu, *Chem. Sci.*, 2011, 2, 1262-1267.

[19] D. Gopalakrishnan, D. Damien, B. Li, H. Gullappalli, V. K. Pillai, P. M. Ajayanb and M. M. Shaijumon, *Chem. Commun.*, 2015, 51, 6293-6296.

[20] D. Merki, H. Vrubel, L. Rovelli, S. Fierro and X. Hu, *Chem. Sci.*, 2012, 3, 2515-2525.

[21] B. Hinnemann, P. G. Moses, J. Bonde, K. P. Jørgensen, J. H. Nielsen, S. Horch, I. Chorkendorff and J. K. Nørskov, *J. Am. Chem. Soc.*, 2005, 127, 5308-5309.

[22] T. F. Jaramillo, K. P. Jørgensen, J. Bonde, J. H. Nielsen, S. Horch and I. Chorkendorff, *Science*, 2007, 317, 100-102.

[23] T. F. Jaramillo, J. Bonde, J. Zhang, B. L. Ooi, K. Andersson, J. Ulstrup and I. Chorkendorff, *J. Phys. Chem. C*, 2008, 112, 17492-17498.

[24] Z. Chen, D. Cummins, B. N. Reinecke, E. Clark, M. K. Sunkara and T. F. Jaramillo, *Nano Lett.*, 2011, 11, 4168-4175.

[25] J. Kibsgaard, Z. Chen, B. N. Reinecke and T. F. Jaramillo, *Nat. Mater.*, 2012, 11, 963-969.

[26] A. B. Laursen, S. Kegnæs, S. Dahla and I. Chorkendorff, *Energy Environ. Sci.*, 2012, 5, 5577-5591.

[27] L. Liao, J. Zhu, X. Bian, L. Zhu, M. D. Scanlon, H. H. Girault and B. Liu, *Adv. Funct. Mater.*, 2013, 23, 5326-5333.

[28] J. Xie, H. Zhang, S. Li, R. Wang, X. Sun, M. Zhou, J. Zhou, X. W. Lou and Y Xie, *Adv. Mater.*, 2013, 25, 5807-5813.

[29] Q. H. Wang, K. Kalantar-Zadeh, A. Kis, J. N. Coleman and M. S. Strano, *Nature Nanotech.*, 2012, 7, 699-712.

[30] X. Zhang and Y. Xie, *Chem. Soc. Rev.*, 2013, 42, 8187-8199.

[31] J. Feng, X. Sun, C. Wu, L. Peng, C. Lin, S. Hu, J. Yang and Y. Xie, *J. Am. Chem. Soc.*, 2011, 133, 17832-17838.

[32] Y. Yu, S. Huang, Y. Li, S. N. Steinmann, W. Yang and L. Cao, *Nano Lett.*, 2014, 14, 553-558.

[33] H. Tang and S. R. Morrison, *Thin Solid Films*, 1993, 227, 90-94.

[34] P. Joensen, R. F. Frindt and S. R. Morrison, *Mat. Res. Bull.*, 1986, 21, 457-461.

[35] G. Eda, H. Yamaguchi, D. Voiry, T. Fujita, M. Chen and M. Chhowalla, *Nano Lett.*, 2011, 11, 5111-5116.

[36] S. M. Yan, W. Qiao, X. He, X. Guo, L. Xi, W. Zhong and Y. W. Du, *Appl. Phys. Lett.*, 2015, 106, 012408: 1-5.

[37] J. P. Wilcoxon, P. P. Newcomer and G. A. Samara, *J. Appl. Phys.*, 1997, 81, 7934-7944.

[38] D. Gopalakrishnan, D. Damien and M. M. Shaijumon, *ACS Nano*, 2014, 8, 5297-5303.

[39] Z. X. Gan, L. Z. Liu, H. Y. Wu, Y. L. Hao, Y. Shan, X. L. Wu and P. K. Chu, *Appl. Phys. Lett.*, 2015, 106, 233113: 1-5.

[40] M. W. Peterson, M. T. Nenadovic, T. Rajh, R. Herak, O. I. Micic, J. P. Goral and A. J. Nozik, *J. Phys. Chem.*, 1988, 92, 1400-1402.

[41] Y. Li, H. Wang, L. Xie, Y. Liang, G. Hong and H. Dai, *J. Am. Chem. Soc.*, 2011, 133, 7296-7299.

[42] D. Merki and X. Hu, *Energy Environ. Sci.*, 2011, 4, 3878-3888.

[43] J. D. Benck, Z. Chen, L.Y. Kuritzky, A. J. Forman and T. F. Jaramillo, *ACS Catal.*, 2012, 2, 1916-1923.

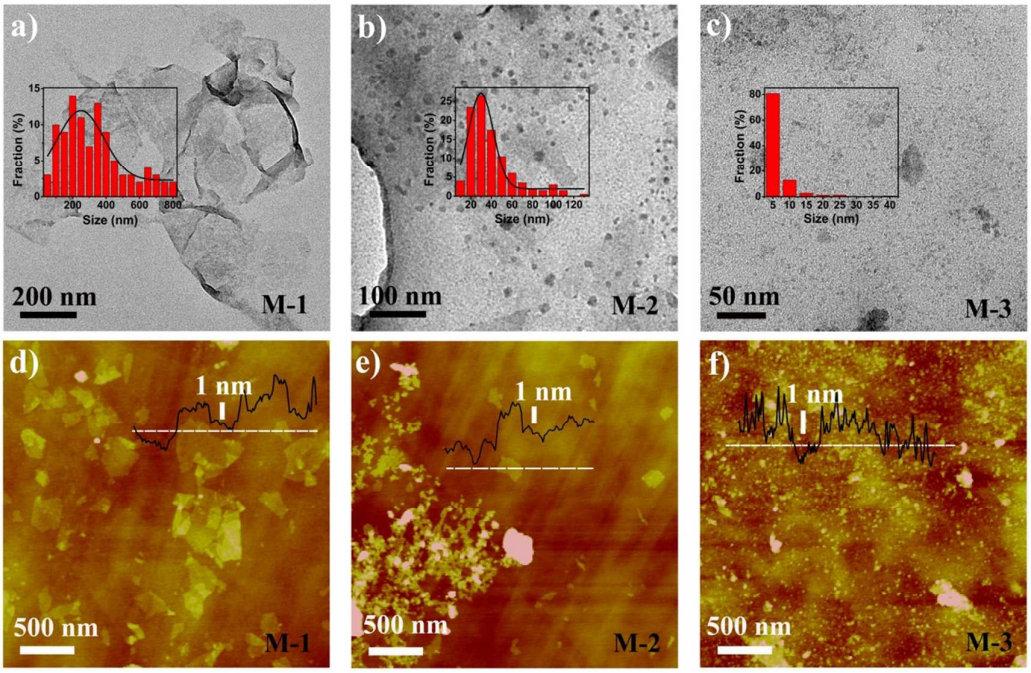

Figure 1. a-c) TEM images and d-f) AFM images of the MoS_2 nanosheets after the first exfoliation (M-1), second exfoliation (M-2) and third exfoliation (M-3), respectively. Insets in a-c) show the lateral size distribution of M-1, 2, 3; Height profiles along the white dashed line are overlaid on the AFM images.

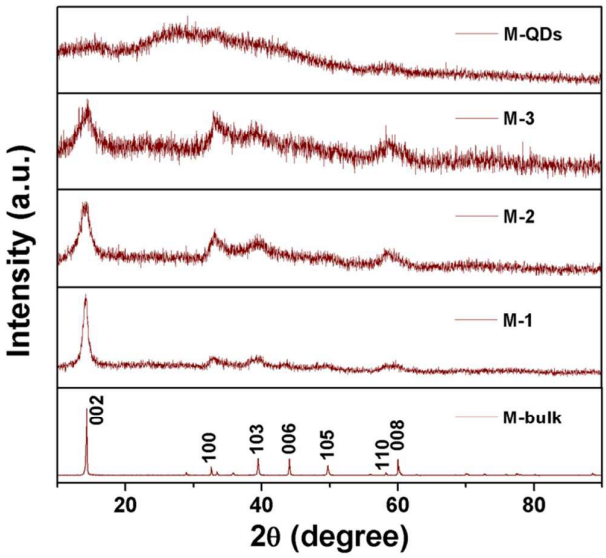

Figure 2. XRD patterns of bulk MoS_2, various MoS_2 nanosheets after each exfoliation and MoS_2 QDs.

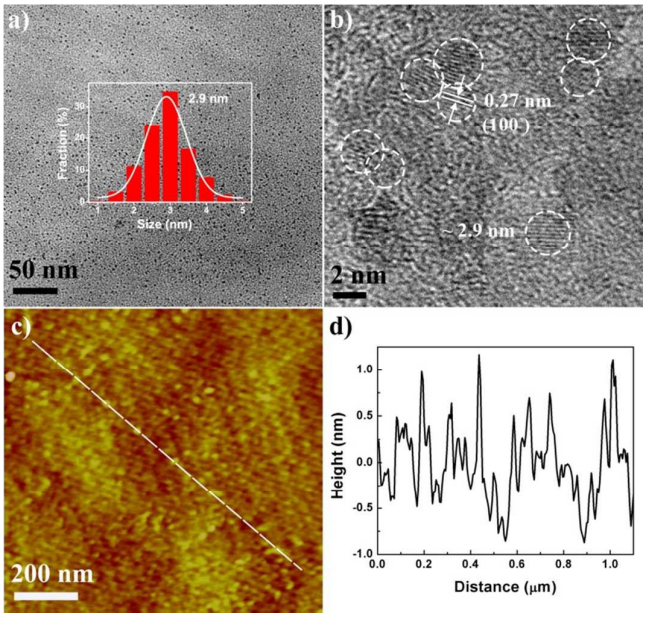

Figure 3. a) TEM image, b) HRTEM image, c) AFM image of the monolayer MoS_2 QDs. Inset in a) shows the lateral size distribution of the MoS_2 QDs. d) Height profile of the MoS_2 QDs along the dashed line shown in c).

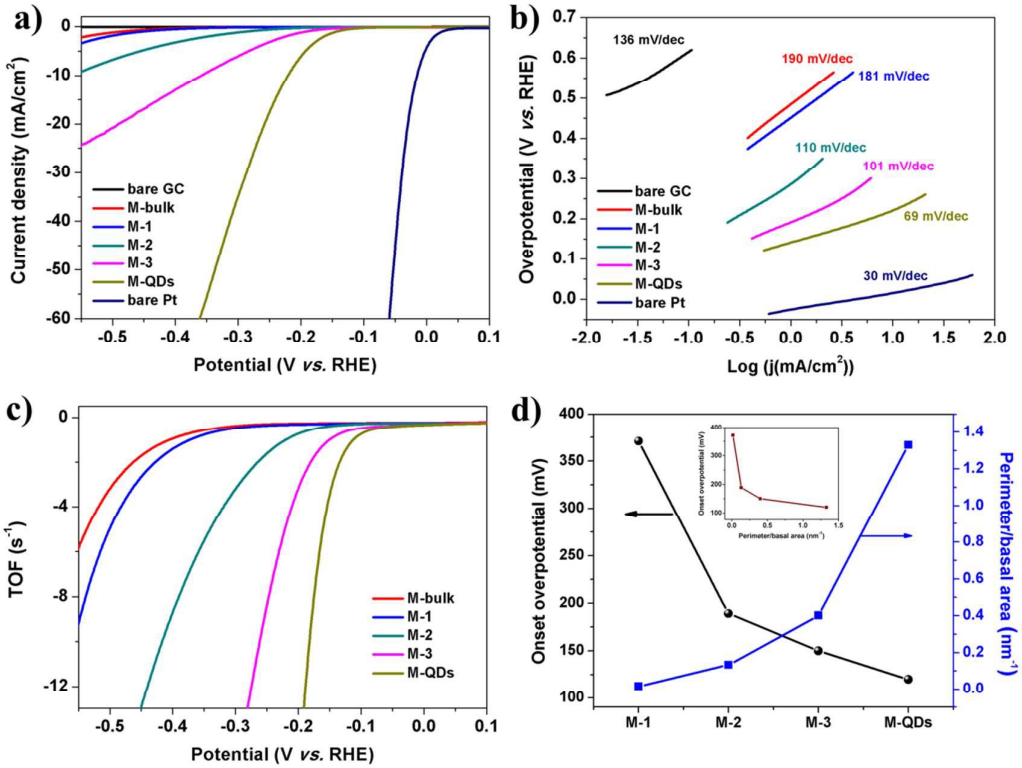

Figure 4. (a) Polarization curves obtained in 0.5 M H_2SO_4 and (b) corresponding Tafel plots of various electrocatalysts. (c) Calculated turnover frequencies (TOF) of various electrocatalysts. (d) The variation of the onset overpotential and the ratio of perimeter to basal area of various samples.

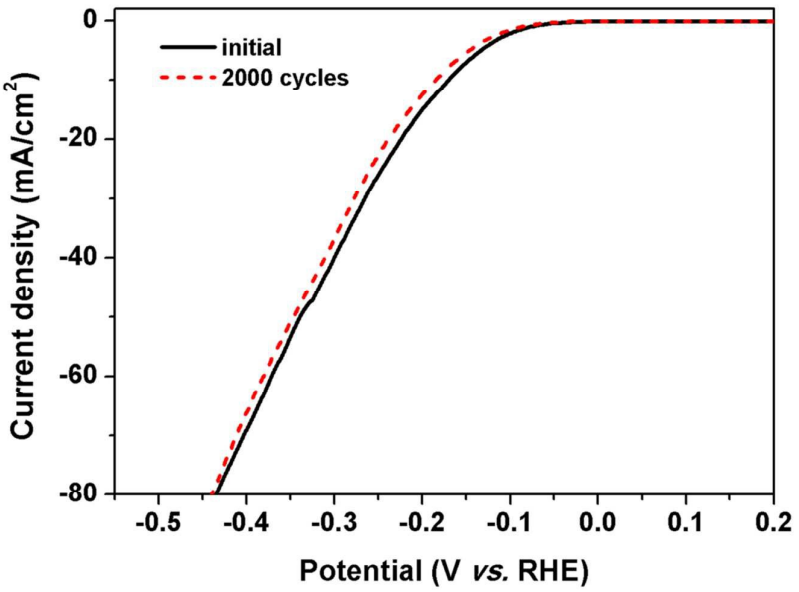

Figure 5. Stability test for the monolayer MoS_2 QDs

Table 1. Electrochemical analysis of various MoS_2 catalysts.

Sample	Perimeter/basal area (nm^{-1})	Onset potential η (mV)	Tafel slope (mV/dec)	j_0 ($\times 10^{-5}$ A/cm^2)	TOF ($\times 10^{-2}$ s^{-1}) based on j_0
M-bulk	-	390	190	0.24	0.64
M-1	~2/125	371	181	0.39	1.05
M-2	~2/15	189	110	1.34	3.60
M-3	~2/5	150	101	1.63	4.38
M-QDs	~2/1.5	120	69	1.79	4.81

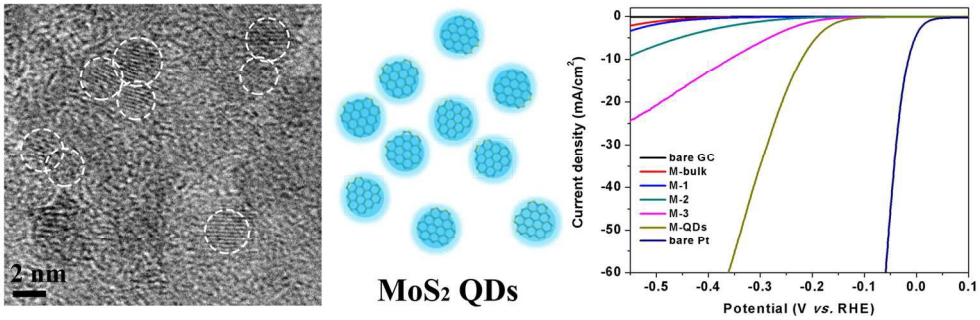

A multi-exfoliation route was used to prepare monolayer MoS2 quantum dots with improved electrocatalytic activity for hydrogen evolution.
150x50mm (300 x 300 DPI)